STUDIA UBB PHYSICA, Vol. 60 (LX), 2, 2015, pp. 89-96
(RECOMMENDED CITATION)

SYNTHESIS, STRUCTURAL CHARACTERIZATION AND *IN VITRO* EVALUATION OF BIOACTIVITY OF SILVER CONTAINING BIOACTIVE GLASSES

R. A. POPESCU[1,2], K. MAGYARI[1], I. PAPUC[2], L. BAIA[1]*

ABSTRACT. Five silver doped SiO_2–CaO–P_2O_5 based bioactive glasses were synthesized and structurally characterized in order to find the optimal concentration that can be further used in scaffold fabrication for bone tissue engineering. Initially, the recorded XRD patterns confirmed the existence of a preponderantly amorphous structure for all samples, though the presence of some crystallization centres associated with tricalcium phosphate phase was also revealed. The UV-vis spectra evidenced signal originated from the surface plasmon resonances of the silver nanoparticles. The signature of both types of isolated and cluster silver nanoparticles were signalized, the amount of the silver aggregates was found to progressively increase starting with 0.5 mol% Ag_2O. Bioactivity assessment was also performed for the obtained samples, and it was determined a good response to all compositions. However, for the sample with 0.5 mol% Ag_2O the content of the self-assembled hydroxyapatite phases was more noticeable and also was taken into consideration the absence of a high signal from AgCl. This can be considered the optimum concentration of silver, from the obtained samples range, that can be further used for scaffold preparation.

Keywords: *XRD, Uv-Vis, bioactivity, silver.*

INTRODUCTION

In the last years, substantial growth has been reported in the area of biomaterials used for tissue reconstruction [1]. A large attention was captured by some bioactive ceramics used as artificial bone grafts, because of their properties

[1] *Faculty of Physics & Interdisciplinary Research Institute on Bio-Nano-Sciences, Babes-Bolyai University, 400084 Cluj-Napoca, Romania.*
[2] *Faculty of Veterinary Medicine, University of Agricultural Science and Veterinary Medicine, 400372 Cluj-Napoca, Romania.*
[*] *Corresponding author e-mail: lucian.baia@phys.ubbcluj.ro*

to form *in vivo* a bone-like apatite layer able to promote the osteoformation [2, 3]. An important feature is their ability to improve revascularization, osteoblast adhesion, enzyme activity, and differentiation of mesenchymal stem cells [4, 5].

This is a domain of intense research, which is distinctly manifested in the rising number of publications in the field of bioactive glasses, their attributes and applications [4, 6]. There are two principal ways to prepare bioactive glasses, namely, the melt quenching method and sol-gel one [7]. Sol-gel derived bioactive glasses are produced by the hydrolysis of organic precursors followed by the polycondensation. Finally the gel is heat treated to form a glass and to remove the organic part [7, 8].

Silver is recognized as an antiseptic agent that was frequently used in diverse implant materials such as bioactive glasses, metallic alloys and polymers [9, 10]. It should be noted that there was no observed cytotoxicity effect for animal cells when silver ion concentrations released were lower than 1.6 mg/L [10-12].

Bioactive glasses containing Ag_2O are attractive materials because they combine antibacterial effect of silver with the glass bioactivity [13, 14]. It is well known that silver ions have positive effect against microbial threat, being very efficient in small quantities [15]. A number of studies revealed that the addition of Ag_2O into bioactive glass decreases the probability of bacterial contamination and does not negatively affect the glass matrix bioactivity [16, 17].

The aim of this study was to produce a wide range of bioactive glasses containing silver, to characterize them and to find the optimal concentration that can be further used in scaffold fabrication for bone tissue engineering. In this regard was made also a bioactivity test to sustain and improve the previously obtained results [18].

EXPERIMENTAL

Synthesis of the glass

The samples belonging to the $60SiO_2 \cdot (32\text{-}x)CaO \cdot 8P_2O_5 \cdot xAg_2O$ (mol%) system with x=0; 0.5; 1; 1.5; 2 and 2.5, were prepared by sol-gel method. The precursors used were tetraethyl orthosilicate (TEOS), triethyl phosphate (TEP), calcium nitrate tetrahydrate ($Ca(NO_3)_2 \cdot 4H_2O$) and silver nitrate ($AgNO_3$) hydrolyzed in the presence of nitric acid; the (HNO_3+H_2O)/(TEOS+TEP) molar ratio was equal to 8. Reactants were added consecutively after 1-hour intervals, under continuous stirring. The solutions (*sols*) were poured into closed containers that were kept at 37°C until gelation (*gels*) was reached (1-2 days). The resultant gels were aged at 37°C for 2 days and it were dried at 120°C for 24 h.

Material stabilization was carried out at 600°C for 3 hours. This temperature was determined by differential thermal analysis of the dried gels. Prior characterization the obtained glass was milled.

Methods

X-ray Diffraction

The X-ray diffraction analysis (XRD) was carried out on a Shimadzu XRD 6000 diffractometer using CuKα radiation (λ=1.54 Å), with Ni-filter. The diffractograms were recorded in 2θ range from 10° to 80° with a speed of 2°/min.

UV-vis Spectroscopy

Absorption measurements of the samples were performed with an Analytic Jena Specord 250 plus UV-Vis spectrometer. The spectral resolution was of 2 nm.

FT-IR Spectroscopy

The FT-IR absorption spectra were recorded with a JASCO 6200 (Jasco, Tokyo, Japan) spectrometer, at room temperature, in the 400–4000 cm^{-1} range with a spectral resolution of 4 cm^{-1} and using the well-known KBr pellet technique. The recorded spectra were smoothed by a 5-point Savitzky-Golay smoothing function for background correction.

Assessment of the bioactivity

In order to check the bioactivity, the obtained powders were immersed in simulated body fluid (SBF), in closable conical polypropylene tubes that were placed in an incubator at a constant temperature of 37 °C, under static condition for 7 days. The SBF was prepared according to Kokubo's protocol [19]. The solution was buffered at a pH of 7.4 at 37°C. The weight of glass per volume of SBF used was 10 mg/ml for each sample. After 7 days, the powders were filtrated, rinsed several times with distillate water, and dried.

RESULTS AND DISCUSSION

Structural Characterization

The XRD patterns disclose the amorphous structure of the samples after heat treatment. However, around 2Θ~32° could be observed some signals associated with a few crystallization centers. These suggest the formation of tricalcium phosphate phase, found as $Ca_3(PO_4)_2$ H_2O [20].

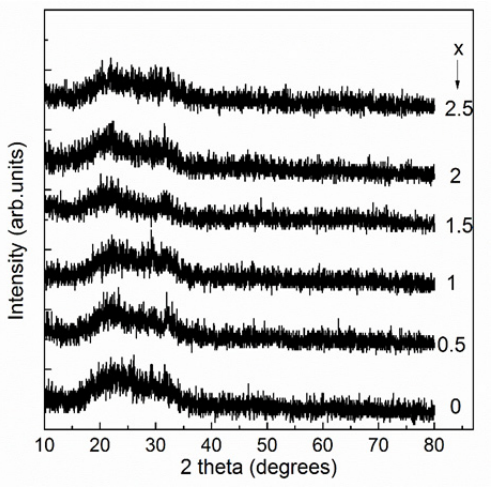

Fig. 1. XRD patterns of the $60SiO_2 \cdot (32\text{-}x)CaO \cdot 8P_2O_5 \cdot xAg_2O$(mol%) samples

In the FT-IR spectra could be observed absorption bands characteristic to Si-O-Si stretching (1040 and 860 cm^{-1}) and Si-O-Si bending vibrations (510 cm^{-1}). Water is displayed on the wide absorption signal around 1640 cm^{-1}. The band at 1440 cm^{-1} indicates the existence of the carbonate group and the 560 and 580 cm^{-1} signals prove the presence of the phosphate groups [20]. The recorded FTIR spectra do not show significant changes. This is most probable a consequence of the low content of Ag_2O.

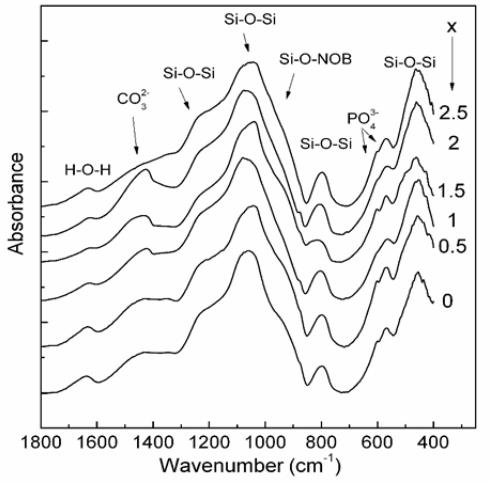

Fig. 2. FT-IR spectra of the $60SiO_2 \cdot (32\text{-}x)CaO \cdot 8P_2O_5 \cdot xAg_2O$(mol%) samples

Uv-vis spectra showed between 300 and 330 nm a signal occurred due to electronic transitions in Ag metallic species [21]. This signal increases in intensity as the silver concentration rises [22]. According to the literature, the silver doped samples could reveal surface plasmon resonance bands in the 400-500 nm as a result of the Ag nanoparticles presence [21, 22]. By analysing our Uv-vis spectra can be observed the occurrence of an absorption signal with a maximum at around 420 nm. This signal is most prominent on x=0.5 mol% Ag_2O sample and is associated with the existence of silver nanoparticles inside the glass matrix [22]. The shape of the band is asymmetric because another signal, which is due to the surface plasmon resonances of the agglomerations of Ag nanoparticles, is convoluted with that given by surface plasmon resonances of the isolated Ag nanoparticles. Once the silver amount increases one can observe a slight shift of the band around 420 nm towards 450 nm, as a consequence of either the increase amount of Ag nanoparticle clusters, or the rising of the silver nanoparticles dimension [21, 22].

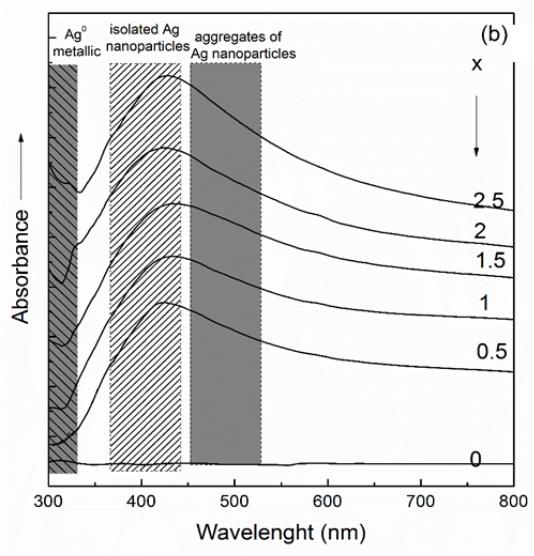

Fig. 3. UV-vis spectra of the $60SiO_2 \cdot (32\text{-}x)CaO \cdot 8P_2O_5 \cdot xAg_2O$(mol%) samples

Assessment of the bioactivity

After 7 days of samples immersion in SBF, the XRD patterns reveals the occurrence of hydroxyapatite (HA) phase between the recorded signals at 2θ~26° and 32°. Likewise could be observed specific signals for silver chloride at 2θ~46°. To easily associate apatite and silver chloride phases, XRD pattern of HA and AgCl are included as references [23, 24] According to the literature, AgCl has no

negative effects on living organisms, moreover it is preferred in detriment of high silver nanoparticles concentration of [25].

In the FT-IR spectra of the samples immersed in SBF, the bands at 604 and 564 cm^{-1} show an almost proportional intensity at each concentration. This indicates a good bioactivity of all samples [20]. However, the sample with 0.5 mol% Ag_2O shows the highest bioactivity potential of all if we are taking into consideration also the absence of a high signal from AgCl.

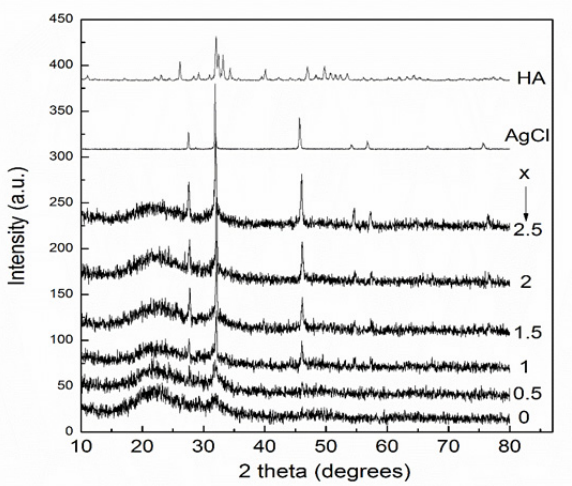

Fig. 5. XRD patterns of the $60SiO_2 \cdot (32\text{-}x)CaO \cdot 8P_2O_5 \cdot xAg_2O$(mol%) samples after immersion in SBF for 7 days. The XRD patterns of HA and AgCl are also included for comparison purpose

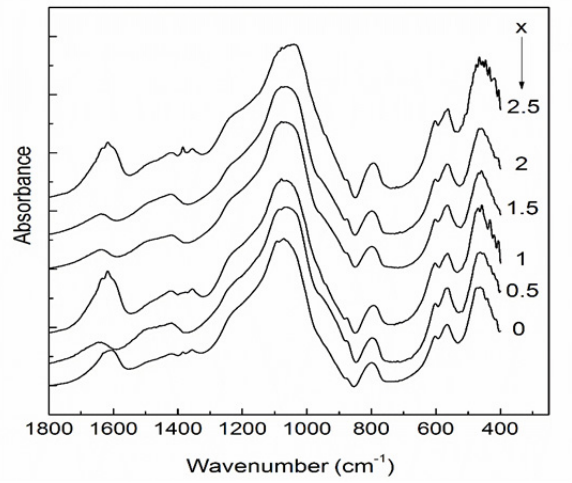

Fig. 6. FT-IR spectra of the $60SiO_2 \cdot (32\text{-}x)CaO \cdot 8P_2O_5 \cdot xAg_2O$(mol%) samples after immersion in SBF for 7 days

CONCLUSIONS

In this paper a wide range of compositions containing silver oxide were synthesized having SiO_2-CaO-P_2O_5 as a base formula. The obtained results guided us to sum the entire range of concentrations to a single one that was the most suitable for our future purposes.

The XRD patterns, FT-IR and UV-Vis spectra show structural characteristics that indicate the bioactive character of all investigated samples. Concentration with x=0.5 mol% Ag_2O proved to be the most suitable because of both the absence of an important amount of AgCl and its bioactive character. Thus, the composition that fits most of the requirements for its further use at scaffold fabrication is 60SiO2·31.5CaO·8P2O5·0.5Ag_2O(mol%).

ACKNOWLEDGMENTS

This paper is a result of a doctoral research made possible by the financial support of the Sectoral Operational Programme for Human Resources Development 2007-2013, co-financed by the European Social Fund, under the project POSDRU/187/1.5/S/155383-“Quality, excellence, transnational mobility in doctoral research”.

REFERENCES

1. M. Catauro, M. G. Raucci, F. D. E. Gaetano, and A. Marotta, *J. Mater. Sci.: Materials in Medicine.* 5, 831 (2004).
2. C. Gruian, A. Vulpoi, E. Vanea, B. Oprea, H.-J. Steinhoff, and S. Simon, *J. Phys. Chem. B*, 117(51), 16558 (2013).
3. C. Balagna, C. Vitale-Brovarone, M. Miola, E. Verne, R. A. Canuto, S. Saracino, G. Muzio, G. Fucale, and G. Maina, *J. Biomater. Appl.*, 25(6), 595 (2011).
4. G. Kaur, O. P. Pandey, K. Singh, D. Homa, B. Scott, and G. Pickrell, *J. Biomed. Mater. Res. Part A*, 102(1), 254 (2014).
5. M. Miola, M. Bruno, G. Maina, G. Fucale, G. Lucchetta, and E. Vernè, *Mater. Sci. Eng. C*, 43, 65 (2014).
6. H. Zhu, C. Hu, F. Zhang, X. Feng, J. Li, T. Liu, J. Chen, and J. Zhang, *Mater. Sci. Eng. C*, 42, 22 (2014).
7. J. R. Jones, L. M. Ehrenfried, P. Saravanapavan, and L. L. Hench, *J. Mater. Sci. Mater. Med.*, 17(11), 989 (2006).

8. M. Catauro, F. Bollino, F. Papale, and S. Vecchio Ciprioti, *J. Non. Cryst. Solids*, 422, 16 (2015).
9. K. Glinel, P. Thebault, V. Humblot, C. M. Pradier, and T. Jouenne, *Acta Biomater.*, 8(5), 1670 (2012).
10. X. Chatzistavrou, J. C. Fenno, D. Faulk, S. Badylak, T. Kasuga, A. R. Boccaccini, and P. Papagerakis, *Acta Biomater.*, 10(8), 3723 (2014).
11. A. R. Shahverdi, A. Fakhimi, H. R. Shahverdi, and S. Minaian, *Nanomedicine Nanotechnology, Biol. Med.*, 3(2), 168 (2007).
12. K. H. Cho, J. E. Park, T. Osaka, and S. G. Park, *Electrochim. Acta*, 51(5), 956 (2005).
13. A. Vulpoi, C. Gruian, E. Vanea, L. Baia, S. Simon, H.-J. Steinhoff, G. Göller, and V. Simon, *J. Biomed. Mater. Res. Part A*, 100A(5), 1179 (2012).
14. S.-H. Luo, W. Xiao, X.-J. Wei, W.-T. Jia, C.-Q. Zhang, W.-H. Huang, D.-X. Jin, M. N. Rahaman, and D. E. Day, *J. Biomed. Mater. Res. Part B Appl. Biomater.*, 95B(2), 441 (2010).
15. K. Magyari, C. Gruian, B. Varga, R. Ciceo-Lucacel, T. Radu, H.-J. Steinhoff, G. Váró, V. Simon, and L. Baia, *J. Mater. Chem. B*, 2(35), 5799 (2014).
16. M. Bellantone, N. J. Coleman, and L. L. Hench, *J. Biomed. Mater. Res.*, 51, 484 (2000).
17. A. Vulpoi, V. Simon, H. Ylanen, and S. Simon, *J. Compos. Mater.*,48(1), 63 (2014).
18. R. A. Popescu, K. Magyari, R. Stefan, I. Papuc, and L. Baia, *Stud. UBB Phys.*, 60(1), 103 (2015).
19. T. Kokubo and H. Takadama, *Biomaterials*, 27(15), 2907 (2006).
20. K. Magyari, L. Baia, A. Vulpoi, S. Simon, O. Popescu, and V. Simon, *J. Biomed. Mater. Res. Part B Appl. Biomater.*, 103B, 261 (2015).
21. L. Baia, D. Muresan, M. Baia, J. Popp, and S. Simon, *Vib. Spectrosc.*, 43(2), 313–318 (2007).
22. K. Magyari, R. Stefan, D. C. Vodnar, A. Vulpoi, and L. Baia, *J. Non. Cryst. Solids*, 402, 182 (2014).
23. Downs RT. The RRUFF Project: An integrated study of the chemistry c, Raman and infrared spectroscopy of minerals. In: Program and Abstracts of the 19th General Meeting of the International Mineralogical Association in Kobe, Japan; 2006. O03–13. RRUFF ID: R060180. http://rruff.info/general5HA/display5default/R060180,
24. Downs RT. The RRUFF Project: An integrated study of the chemis-try c, Raman and infrared spectroscopy of minerals. In: Program and Abstracts of the 19th General Meeting of the International Mineralogical Association in Kobe, Japan; 2006. O03–13. RRUFF ID: R050360, http://rruff.info/chem=Cl,Ag/display=default/R050360
25. S. Zhang, C. Du, Z. Wang, X. Han, K. Zhang, and L. Liu, *Toxicol. Vitr.*, 27(2), 739 (2013).